Velocity calibration and wavefield decomposition for walkover VSP data

Markus von Steht and Jürgen Mann, *Geophysical Institute, University of Karlsruhe*

SUMMARY

Generalized stacking velocity analysis tools like the Common-Reflection-Surface stack method provide stacking parameters beyond the conventional stacking velocity. Although initially given in terms of first and second traveltime derivatives, these parameters can be expressed in terms of useful geometrical wavefront properties. However, this geometrical interpretation requires a good estimation of the tuned velocities which are valid for imaging in the vicinity of source and/or receiver of the recorded data. Using the downgoing first arrivals, we introduce a simple and efficient method to determine the velocities at every receiver level in a walkover VSP experiment. The hereby calibrated wavefront properties are exemplarily used for the decomposition into upgoing waves arriving either as P- or S-waves at the receivers.

INTRODUCTION

The Common-Reflection-Surface (CRS) stack method and similar stacking approaches can be seen as generalized stacking velocity analysis tools. In contrast to conventional stacking velocity analysis, these methods provide entire sets of stacking parameters which carry useful information for a variety of applications like inversion. The generalized stacking parameters can be interpreted in several ways (see, e. g., Hertweck et al., 2007): in the data, they can be observed as the first and second spatial derivatives of traveltime. Alternatively, these can be expressed in terms of slowness components and imaging velocities, including the classic stacking velocity for the zero-offset case. Another attractive means of interpretation is to relate the traveltime derivatives to properties of (hypothetical) wavefronts, namely their propagation directions and curvatures at the source and the receiver, respectively. In particular the wavefront propagation directions—usually quite stable parameters—can be employed for various purposes, e. g. topography handling, redatuming, and wavefield separation on multi-component data (see, e. g., Zhang, 2003; Boelsen and Mann, 2005).

In order to relate the traveltime derivatives to this geometrical interpretation, we need a good estimation of the *tuned* velocities in the vicinity of the respective source and/or receiver for which the derivatives were calculated. For the application of the CRS stack, these velocities are usually assumed to be known and considered as virtually constant within the local stacking aperture. As long as the geometrical interpretation is not explicitly used within the stacking process itself, the accuracy of the velocities is not crucial and a calibration of the wavefront properties with more accurate velocities can be applied later on. In ordinary CRS processing, the geometrical interpretation enters only via extremal emergence angles which are convenient to constrain the search range for the first derivatives. If the velocity is underestimated, the search range will be larger and more coarsely sampled than intended. Too high velocities will have the opposite effect, in the worst case leading to the loss of steep events. It can be shown that in case of doubt, an underestimated velocity will not introduce failures due to inaccuracies but only a slight computational overhead.

If the geometrical interpretation comes into turn, the accuracy becomes far more critical, especially in case of wavefront propagation directions being used to discriminate differently polarized wave types in multi-component data. As shown by Boelsen and Mann (2005) the CRS method can be extended to handle multi-component data by using the operator shape and orientation simultaneously with polarization directions. With inaccurate velocities the orientation of wavefronts emerging at the receivers and, thus, also the polarization directions are wrongly estimated and the results are deteriorated: the different wave types will appear intermixed rather than separated. Another example for processes sensitive to the accuracy of the velocity is the handling of topography in surface seismics or deviated wells in VSP acquisition. Here, the propagation direction is implicitly used to redatum the data to more convenient reference levels. A biased estimate of this propagation direction will evidently lead to lateral and temporal displacement of the redatumed reflection events.

CRS STACK FOR VSP GEOMETRIES

A typical survey method which features multi-component acquisition are VSP experiments. Compared to surface seismics, the superior receiver-coupling and the absence of weathering zone and free surface in the well allow the direct observation of the polarization of emerging body waves. Here, the geometrical interpretation of stacking parameters is very convenient, e. g. for wavefield decomposition. Furthermore, walkover VSP data allow to easily calibrate the velocities for all receiver levels from the kinematics of the wavefield. We will introduce this concept quite generally for the 3D case and a vertical borehole and additionally provide an assessment with respect to deviated wells. We will present an application of this calibration method to a synthetic VSP walkover line with a vertical well and apply the calibrated propagation directions for wavefield decomposition.

The CRS traveltime approximation used for VSP processing is a variation of the CRS approach for *finite-offset* surface seismic data by Zhang et al. (2001) with an extension to general acquisition geometries (one possible solution can be found in Boelsen and Mann, 2005; Boelsen, 2005). We do not want to go into any details concerning the actual traveltime approximation being employed. In the context of this paper it is sufficient to know that source and receiver positions will, in general, not coincide. Thus, the approximation depends on two components of the traveltime gradient with respect to either position. Due to the limitations of borehole acquisition we can only determine one component on the receiver side from VSP data.
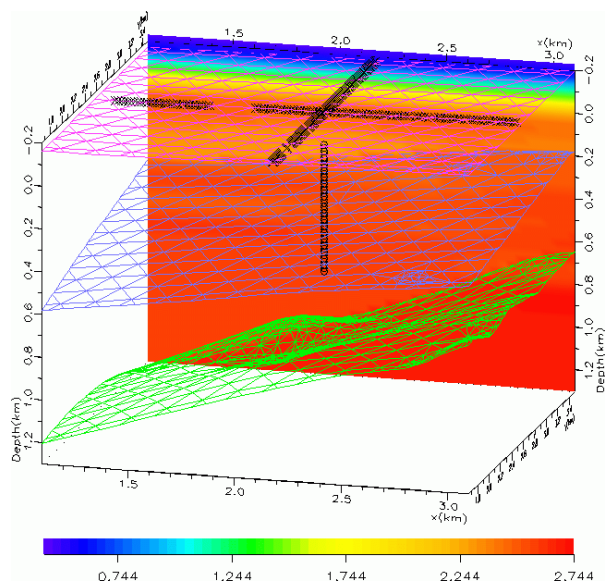
Figure 1: Geometry of receiver levels in the well (circles), source lines (crosses), and triangulated reflectors. A vertical slice through the P-wave velocity model [km/s] is shown in the background.

VELOCITY CALIBRATION

For isotropic media, the propagation direction of a wavefront is normal to the wavefront itself. Furthermore, body waves are polarized either in propagation direction or in the plane tangent to the wavefront. The slowness vector $\vec{p}$ fully characterizes all these directions in this case. However, from the first derivatives of traveltimes, we can only determine up to two components of this vector as the receivers usually cover an acquisition surface rather than an entire volume. For the more particular case of VSP data, the situation is even worse: we are looking for the velocities in the vicinity of the receivers. Due to the one-dimensional nature of a well, the data only provides us with one component of the slowness vector, namely its component p_t tangent to the well.

For a given receiver at (x_G, y_G, z_G) the local velocity v_G is fixed. In general, the waves from different source (and reflection) points will arrive there with different propagation directions, i.e. slowness vectors $\vec{p}$. Thus, the slowness component p_t tangent to the well will vary systematically: for a wave propagating normal to the well it will vanish, for a wave tangent to the well it will reach its maximum: $p_t = |\vec{p}| = v_G^{-1}$. This maximum is the inverse of the *true* velocity v_G, as p_t is the only non-vanishing component of the slowness vector $\vec{p}$ in this case. Note that the latter case does not necessarily occur within the considered combination of given model and chosen acquisition geometry.

Let us now consider the direct downgoing wave in a walkover VSP configuration for a vertical well: here we can expect to have a wide range of propagation directions available which are mainly distributed around the vertical orientation at each receiver. For a sufficiently dense source spacing and suffi-
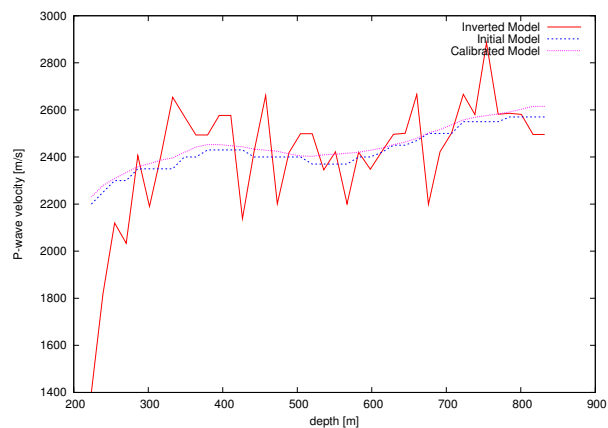

Figure 2: Interval velocities along the well from checkshot inversion (red), underestimated initial model for calibration (blue), and calibrated velocities (magenta).

ciently large acquisition area, it is very likely that at least one of the associated rays will be virtually tangent to the vertical well. Therefore, we can expect that we will actually observe a maximum of the slowness component $p_{t,\max}$ which represents the inverse of the sought-for true velocity v_G. For its determination, we propose the following strategy:

- identification of the downgoing first arrivals
- for each source and each receiver combination contained in the data, determine the tangential slowness component p_t by means of coherence analysis along these events
- for each constant receiver level, search for the source location $(x_S, y_S, 0)$ associated with the maximum tangent slowness component $p_{t,\max}(x_S, y_S; x_G, y_G, z_G)$

In this way, we can determine the velocity $v_G(x_G, y_G, z_G)$ in the vicinity of each particular receiver. For the 2D case shown below, p_t reduces to a function of one source coordinate. Note that in the 3D case, the slowness vector can only be decomposed into a horizontal and a vertical component. The orientation of the horizontal component can e.g. be deduced by means of vectorial coherence criteria using all data components rather than from wavefront properties, only.

DATA EXAMPLE

Modeling

Figure 1 shows a 3D plot of two walkover lines crossing a vertical borehole in N-S and E-W direction, respectively. The acquisition surface is almost planar with a slight dip towards the West. The model contains two reflectors in depths of approximately 0.5 km and 1.0 km. Both are strongly dipping and the second reflector has a very irregular shape. The inhomogeneous elastic background model contains a steep velocity gradient for the first 300 m which cannot be directly observed in the figure because it is clipped out of the displayed range.

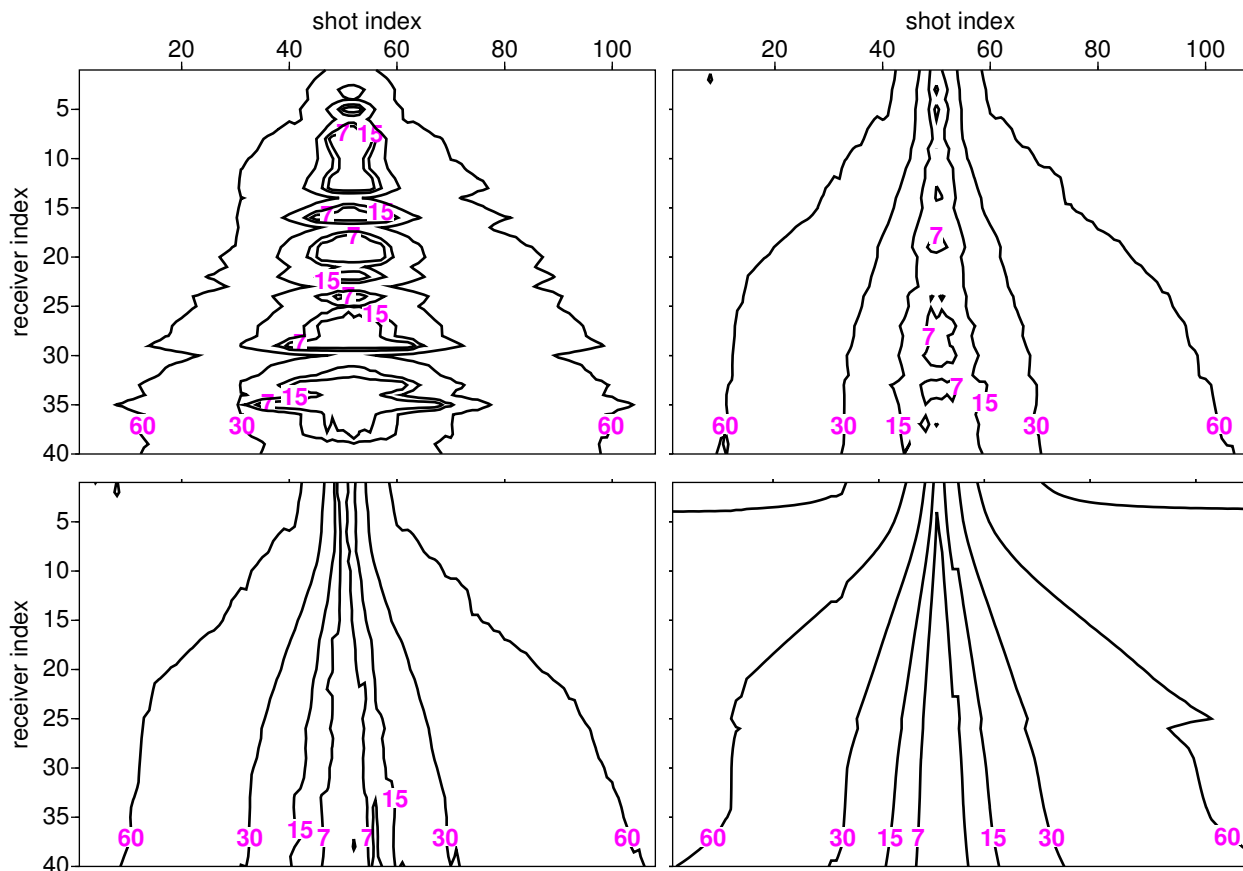## Velocity calibration and wavefield decomposition for walkover VSP data

Figure 3: Isocline representation of receiver emergence angles [°] with respect to the well for every shot/receiver pair computed with interval velocities from check shot inversion (top left), underestimated interval velocities (top right), and calibrated velocities (bottom left). The corresponding ray tracing results are shown on the bottom right.

The corresponding S-wave velocity and density models are not displayed.

By means a wavefront construction method, we have forward-calculated the following wave types for the described model and acquisition geometry:

- downgoing P waves
- reflected PP waves
- reflected SS waves
- converted PS waves

Velocity calibration
In the following, we consider the N-S line, only. For this 2D walkover line, it is more convenient to display the emergence angle β_G with respect to the well rather than the tangent slowness p_t. The first available interval velocity curve was obtained by checkshot inversion (see Figure 2). It served to calculate the emergence angles β_G from the slowness values p_t obtained by coherence analysis in the prestack data. The respective results visualized by means of isoclines in Figure 3 (top left) show that for most receiver levels either a largely under- or over-estimated velocity was chosen. Angle ranges for near-offsets

which either reach a minimum value far from being 0° or re-main at 0° for a wide range clearly indicate either case. By extrapolation of velocities from locations where a reasonably small distinct minimum still can be observed towards uncertain receiver positions we can estimate a preliminary, generally slightly underestimated, depth-velocity curve. The calibration based on this model already results in more consistent emergence angles as shown in Figure 3 (top right).

Now we perform the calibration as proposed above which provides us with the estimation of the tuned depth-velocity curve (see Figure 2). The angles calculated with these velocities are in good agreement with the forward-calculated values of β_G, see Figure 3 (bottom). For this synthetic example, the corresponding tuned velocity curve for S-wave arrivals was computed by simply applying the ratio $v_P/v_S = \sqrt{3}$ as used for the modeling of the data.

Wavefield separation
With the already introduced assumption of a virtually constant velocity in the vicinity of each individual receiver, we can now employ the calibration velocities for subsequent imaging steps to calculate the emergence angles from CRS attributes for various types of reflection events. An obvious and attractive ap-

Velocity calibration and wavefield decomposition for walkover VSP data
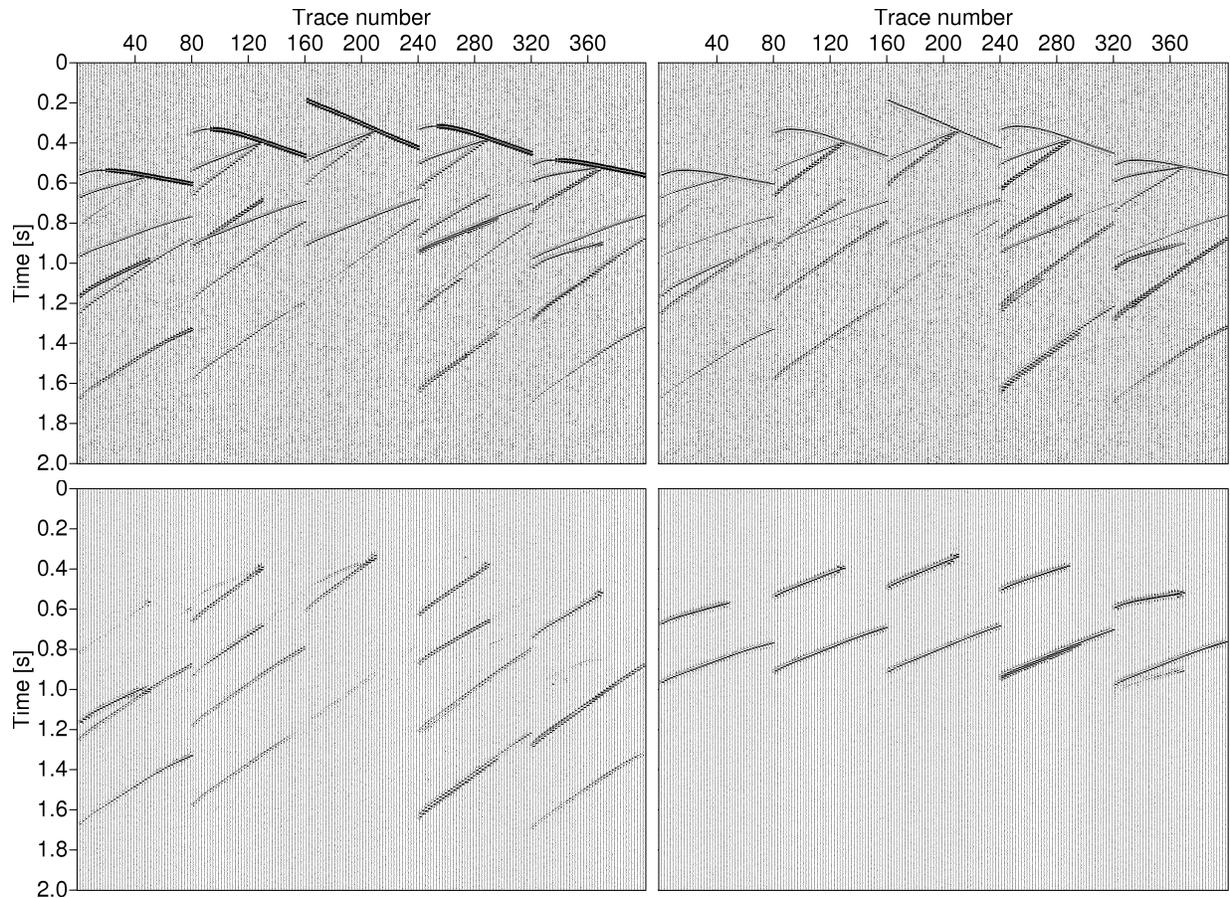

Figure 4: Top: vertical (left) and inline horizontal (right) component of the recorded wavefield. Bottom: transversal (left) and radial (right) component after wavefield decomposition. The orientation of the latter two components depends on the position and the wave type encountered there. Thus, they are generally not mutually orthogonal.

plication of these emergence angles is to perform a wavefield decomposition of the multicomponent data into arriving P- and S-waves. Figure 4 demonstrates the accuracy of the angles: they are very close to the actual polarization direction such that the decomposition works almost perfectly for the considered isotropic model. Each event appears either in the transversal or the radial component.

DEVIATED WELLS

Although presented for a vertical well in this paper, the approach can be easily extended to deviated wells as well. We simply have to introduce a well-centered coordinate system. Again, the ray being tangent to the well at the receiver is associated with the searched-for velocity. However, for strongly deviated wells, the calibration approach might fail: the acquisition geometry might not cover the source position associated with the searched-for ray which reaches the receiver tangent to the well. In other words, the global slowness maximum cannot be found in the data. If we can only detect a supremum rather than a maximum, this clearly indicates such a situation where a calibration is impossible without a risk of misinter-

pretation. For complex models, local maxima might occur. A misinterpretation and, thus, wrong calibration will be the consequence when such a local maximum happens to coincide with the slowness supremum.

CONCLUSIONS

We discussed an approach to recover the tuned velocities for downhole receivers by means of a data-oriented analysis of the slowness component tangent to the well. We used the downgoing direct waves of walkover VSP experiments to determine the modulus of the slowness vector and, thus, the velocity. Integrated into the CRS imaging workflow, we demonstrated the application of the calibrated velocities for wavefield decomposition in synthetic 2D VSP data.

ACKNOWLEDGMENTS

Velocity calibration and wavefield decomposition for walkover VSP data

REFERENCES

Boelsen, T. (2005). The Common-Reflection-Surface Stack for arbitrary acquisition geometries and multi-component data – Theory and Application. Master's thesis, University of Karlsruhe. http://www.wit-consortium.de.

Boelsen, T. and Mann, J. (2005). 2D CO CRS stack for multi-component seismic reflection data. In *Extended abstracts, 67th Conf.* Eur. Assn. Geosci. Eng. Session P063.

Hertweck, T., Schleicher, J., and Mann, J. (2007). Data-stacking beyond CMP. *The Leading Edge*, 26(7):818–827.

Zhang, Y. (2003). *Common-Reflection-Surface Stack and the Handling of Top Surface Topography*. Logos Verlag, Berlin.

Zhang, Y., Bergler, S., and Hubral, P. (2001). Common-Reflection-Surface (CRS) stack for common-offset. *Geophys. Prosp.*, 49(6):709–718.